Materials Science Forum Vols. 636-637 (2010) pp 523-530
© (2010) Trans Tech Publications, Switzerland
doi:10.4028/www.scientific.net/MSF.636-637.523

Effect of Carbon Equivalent on Graphite Formation in Heavy-Section Ductile Iron Parts

J. Lacaze[1,a], S. Armendariz[2,b], P. Larrañaga[3,c], I. Asenjo[3,d], J. Sertucha[3,e] and R. Suárez[3,f]

[1] CIRIMAT, Université de Toulouse, ENSIACET, BP 44362, 31432 Toulouse cedex 4, France

[2] TS Fundiciones, S.A. Pol. Sansinenea Erreka, E-20749 Arroa-Zestoa (Gipuzkoa), Spain

[3] Engineering and Foundry Department, AZTERLAN, Aliendalde auzunea 6, E-48200 Durango (Bizkaia), Spain

[a]jacques.lacaze@ensiacet.fr, [b]sarmendariz@tsfundiciones.com, [c]plarranaga@azterlan.es, [d]iasenjo@azterlan.es, [e]jsertucha@azterlan.es, [f]rsuarez@azterlan.es

Keywords: Ductile iron, Heavy castings, Chunky graphite, Carbon equivalent, Cooling curve.

Abstract. The influence of post-inoculation and of cerium and antimony additions on the solidification process and on the formation of chunky graphite in ductile iron heavy-section parts have been studied previously in the case of near-eutectic alloys. It appeared of interest to complement these works by analysing the effect of carbon equivalent on graphite degeneracy. In the present work, hypo-, hyper- and near-eutectic melts have been cast in large blocks and standard cups. Analysis of the corresponding cooling curves recorded during solidification as well as microstructure observations on these casts have been carried out. A clear effect of carbon equivalent as promoter of chunky graphite formation is observed. The results have been added to the set of data already available and various correlations are discussed.

Introduction

The solidification process of heavy-section parts made of nodular cast iron attracts interest for heavy automotive parts and for wind-mill hubs. The large sections of such castings lead to very slow solidification so that the material is prone to present degenerate graphite [1, 2] that lowers the mechanical properties of the parts. One of the most critical forms of degenerate graphite is chunky graphite, denoted CHG in the following. It consists of large cells, typically 0.5 to 2 mm in diameter, of austenite embedded in a three-dimensional interconnected network of graphite [3]. In a series of previous papers [4-7], metallographic observations on large cast blocks and analysis of the cooling curves recorded during their solidification were presented. For the near-eutectic melts investigated, it has been found that post-inoculation increases the tendency for chunky graphite formation [4], and it was postulated that the opposite trend sometimes reported in the literature [2] was related to the use of chills. Analysis of the cooling curves recorded during solidification of these blocks showed that the solidification proceeds totally below the stable eutectic temperature and may be described in three successive steps [5, 6]: i) formation of primary graphite nodules that grow freely in the melt; ii) precipitation of austenite that grows as dendrites encapsulating the primary nodules, thus leading to a so-called initial eutectic reaction; and iii) bulk eutectic reaction where the remaining melt solidifies giving the usual nodular structure. This is during this latter step that CHG cells may appear. Casting of blocks with or without addition of Sb confirmed the positive effect of this element in avoiding CHG formation [7]. In the present work, castings made with hypo-, hyper- and eutectic melts were carried out in order to investigate the role of the carbon equivalent that has been reported to increase the tendency for CHG formation. The results obtained are compared to previous data.

Experimental

In the present study, three different melts (denoted as trials #9, #14 and #15) were prepared with the aim to obtain hypo-, hyper and near-eutectic alloys. From each of these melts, three cubic blocks 30 cm in size were cast, together with thermal analysis (TA) standard cups and medals for chemical analysis. The methodology followed for preparing all melts, casting blocks and sampling has been fully described previously [4]. The nodularizing treatment has been performed using a FeSiMg ferroalloy (45% Si, 0.9% Al, 2.8% Ca, 9% Mg and 1% rare earths, in weight). All three blocks of each trial were simultaneously cast in the same mould. In Table 1, the blocks are labelled as M5-X-Y, where M5 is for the so called thermal modulus i.e. the ratio between the area and the volume of the block (5 cm), X is the melt number and Y relates to additions made in the gating system of each block (N for no post-inoculation, I for post inoculation). Post-inoculation was performed by adding 0.18% of the weight of the block of a commercial inoculant (70-75% Si, 3.2-4.5% Al, 0.3-1.5% Ca, ~0.3% RE, in weight). Possible additions of pure Sb or of Si by means of a FeSi master alloy (76% Si, 0.5% Al, 0.5%Ca, 0.05% rare earth, in weight) are indicated as Sb and Si respectively at the end of the blocks label. The chemical analyses of the materials are reported in Table 1, together with the carbon equivalent C_{eq} and the stable eutectic temperature T_{eut} calculated according to formula given elsewhere [8]. Cooling curves were recorded from standard TA cups and from a thermocouple located at the centre of each block. After casting, all the blocks were cut and then analysed so as to evaluate the fraction V_V of the blocks affected by CHG and to quantify the nodule count, N_{block}, and the local surface area of chunky graphite, A_A, at the centre of the blocks as previously described [4]. The occurrence of graphite flotation was also checked by metallographic observations.

Table 1. Chemical composition (wt. %) of the alloys, carbon equivalent (wt. %) and stable eutectic temperature (°C).

block	C	Si	P	S	Cu	Mg	Ce	La	Sb*	C_{eq}	T_{eut}
M5-9N	3.65	1.92	0.018	0.014	0.02	0.039	0.0029	0.0020	---	4.19	1162.1
M5-9I											
M5-9ISi		2.33*								4.30	1163.9
M5-14N	3.82	2.41	0.035	---	0.03	0.055	0.0028	0.0024	---	4.49	1164.2
M5-14I											
M5-14ISb									0.008		
M5-15N	3.13	2.08	0.030	0.002	0.02	0.042	0.0026	0.0021	---	3.71	1162.8
M5-15I											
M5-15ISb									0.008		

* Chemical composition was determined on the blocks.

Results

Figure 1 shows a micrograph from the central part of the hyper-eutectic casting M5-14I. The microstructure shows the same features than those observed in near-eutectic alloys with: i) large (primary) nodules embedded in dendrite-like ex-austenite; ii) CHG cells that present very fine graphite precipitates; and iii) an usual structure of nodular iron with (secondary) nodules much smaller than the primary ones. The microstructure of the hypo-eutectic alloy differed only by the larger amount of dendrite-like austenite. Table 2 lists the results of the values of V_V, A_A and N_{block} and indicates if flotation was observed or not. As for near-eutectic alloys previously studied, it is seen that post-inoculation favours the formation of chunky graphite in all cases. The addition of FeSi to the melt (M5-9ISi) increases also the amount of CHG, and this may be possibly because of the associated marked increase in nodule count. As expected, addition of Sb decreases, or even suppresses in the present case, graphite degeneracy. It is seen that the highest V_V value are obtained in the case of the hypereutectic melt, for both post-inoculated and non post-inoculated blocks. As already observed [4], the A_A values do not follow the evolution of V_V, generally changing more erratically. This effect of the carbon equivalent may be tentatively related to the fact that the

fraction of austenite that precipitates as dendrites decreases when C_{eq} increases. Finally, flotation appeared mainly in blocks made of hypereutectic melt.

Table 2. Microstructure data.

Block	A_A [%]	V_V [%]	N_{block} [mm^{-2}]	Flotation
M5-9N	10	1.9	47	No
M5-9I	28	4.3	75	Yes
M5-9ISi	39	6.1	135	No
M5-14N	10	11.1	50	Yes
M5-14I	10	17.6	88	Yes
M5-14ISb	0	0	100	Yes
M5-15N	0	0	31	No
M5-15I	5	7.2	75	No
M5-15ISb	0	0	75	No

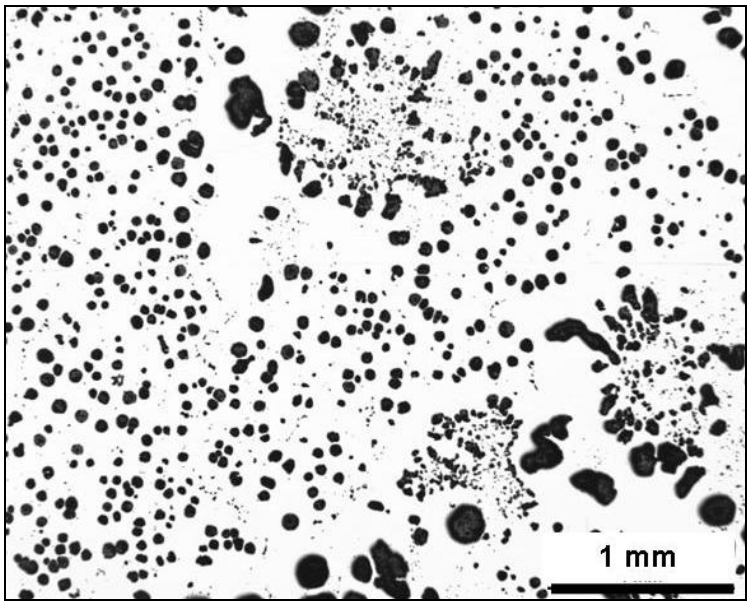

Fig. 1. Micrography at the centre of block M5-14I.

Figure 2 compares the cooling curves obtained with TA cups for non post-inoculated melts cast during trials #14 (hyper-eutectic) and #15 (hypo-eutectic). The record for the former alloy shows clearly the three arrest temperatures, the liquidus, the initial eutectic reaction and the bulk eutectic plateau. As described previously [6] and illustrated in Fig. 2, the corresponding characteristic temperatures are defined as T_L and T_{EN} for the first two arrests, T_{EU} and T_{ER} for the minimum and maximum bulk eutectic temperatures. When the first arrests show recalescence, superscripts 1 and 2 are added for labelling the respective minimum and maximum temperatures. The temperatures evaluated on the TA cups and blocks are listed in Table 3. In case the T_L or T_{EN} arrests could be identified but do not show recalescence, only the temperature at the inflexion point is given. In case these arrests were too faint to be observed, no temperature is reported. Recalescence during the

eutectic reaction may be defined either as bulk eutectic recalescence $\Delta T=(T_{ER}-T_{EU})$ or as the maximum eutectic recalescence $\Delta T_{max}=(T_{ER}-T_{min})$ where T_{min} is the lowest of T_{EN} and T_{EU} values.

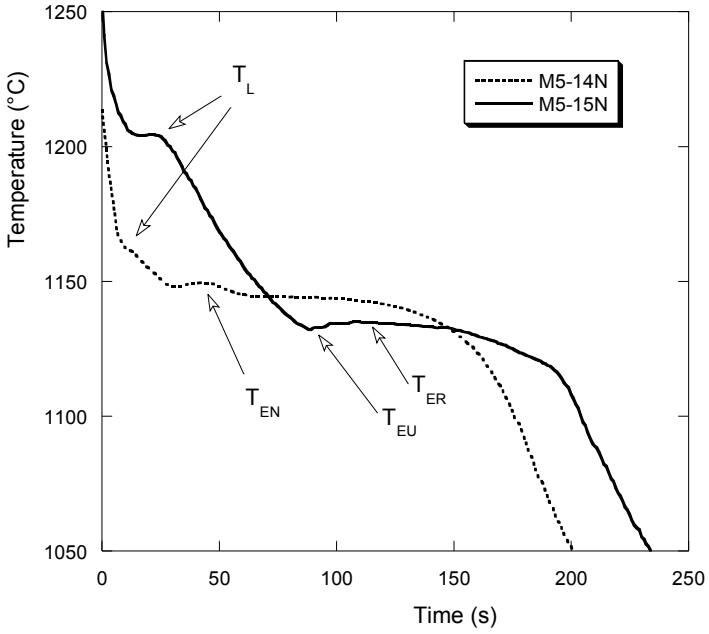

Fig. 2. Cooling curves recorded from the TA cups cast with non post-inoculated #14 and #15 melts. The characteristic temperatures considered in this work are indicated. As no recalescence showed up during the bulk eutectic reaction of M5-14N TA-cup, the T_{EN} and T_{EU} values were taken equal to the temperature at the inflexion point at the very beginning of the eutectic plateau.

Table 3. Characteristic temperatures (°C) evaluated on TA cups and blocks.

Trial	TA cups						Blocks					
	T_L^1	T_L^2	T_{EN}^1	T_{EN}^2	T_{EU}	T_{ER}	T_L^1	T_L^2	T_{EN}^1	T_{EN}^2	T_{EU}	T_{ER}
M5-9N					1138.6	1144.0		1153.8			1147.4	1152.9
M5-9I					1140.4	1146.4		1156.1	1149.3	1154.3	1154.3	1155.1
M5-9ISi								1159.0			1153.0	1158.4
M5-14N		1162.5	1148.2	1149.4		1144.0		1170.0			1156.9	1161.0
M5-14I					1153.0	1157.8		1167.3			1159.4	1161.2
M5-14ISb								1166.3			1160.2	1162.0
M5-15N		1204.2			1132.5	1134.9	1216.1	1217.0			1155.1	1155.2
M5-15I		1203.0			1147.6	1150.0	1213.3	1214.7			1153.2	1153.3
M5-15ISb								1215.1			1158.4	1158.8

The curves recorded on the blocks did show the same overall features than the corresponding TA cup records, with however T_{EU} and T_{ER} values significantly higher in the former case than in the latter as already reported [6]. In the case of the hypo-eutectic alloy, the low carbon equivalent leads to an important primary deposition of austenite, and thus to a eutectic plateau that is much shorter than for the eutectic and hyper-eutectic alloys. Accordingly, bulk eutectic recalescence was lower

for the hypo-eutectic alloy. The main difference between the thermal records for near-eutectic and hyper-eutectic alloys was that the temperature of the bulk eutectic reaction was slightly lower for the former that for the latter ones.

Discussion

The data from the present experimental study is now added to the results obtained previously from near-eutectic melts. Emphasis is put on the relationships discussed previously with the aim at checking if they may be extended to hypo- and hyper-eutectic alloys.

For the near-eutectic melts investigated so far, it has been possible to show experimentally that chunky graphite cells nucleate and grow during the bulk eutectic reaction [5, 7]. Owing to the higher growth rate of these cells as compared to the kinetics of spheroidal graphite eutectic [9], it was expected that the formation of CHG should lead to an increase of bulk eutectic recalescence ΔT. The data available is plotted in Fig. 3 as V_V values versus ΔT, where the results from the present study are shown with larger symbols than the previous ones. It is seen that the whole set of data gives a large cloud of scattered points, though post-inoculated alloys without Sb addition (solid circles) do clearly relate with higher V_V values, as stressed with the full line. This graph could be understood as showing an increase of ΔT with V_V, though with a different sensitivity for post inoculated alloys than for the other ones (non post-inoculated and Sb treated).

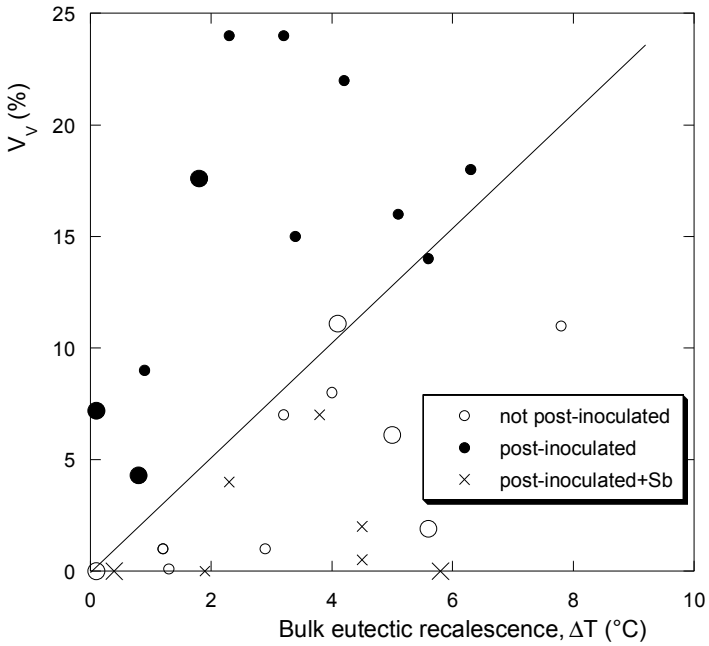

Fig. 3. Correlation between recalescence during bulk eutectic reaction and V_V values.

The trend shown in Fig. 3 is somehow in contradiction with the expected one. Surprisingly, it was possible to find a much less scattered evolution of the data in plotting V_V versus ΔT_{max}, as shown in Fig. 4. The correlation obtained showed an increase of ΔT_{max} from zero to a maximum value of 6-8°C at V_V equal to 10-15%, then a continuous decrease at higher values of V_V. This has been understood as due to the fact that the temperature of the blocks is homogeneous during most of the solidification, so that the effects of early formation of CHG are smoothed out by the larger volume of metal to be reheated [6]. Accordingly, it is thought that a quantitative description of the solidification of the blocks through micro-macroscopic numerical simulation could explain the graph in Fig. 3 because the T_{EU} temperature is lower for non post-inoculated blocks. It should be noted also in Fig. 4 that the correlation does not apply to highly hypo-eutectic alloys as stressed with the arrow that points the data from the inoculated low-carbon alloy.

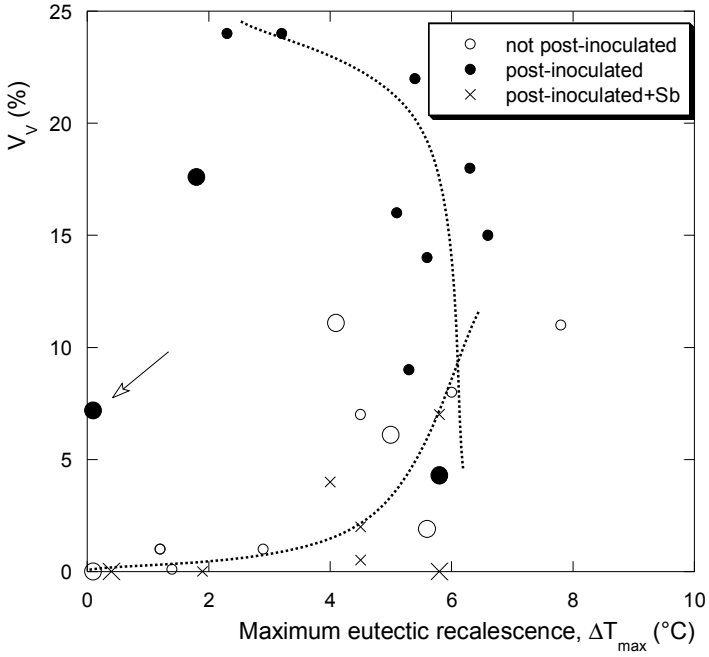

Fig. 4. Plot of V_V versus ΔT_{max} measured on blocks (the arrow indicates the point related to the post-inoculated hypo-eutectic alloy).

Another interesting result was that a correlation could be made between V_V values on blocks and ΔT measured on the TA cups. It is illustrated in Fig. 5 where it is seen a decrease of V_V with ΔT for post-inoculated alloys, and the opposite trend for non post-inoculated ones. The two points marked with arrows are from hypo- and hyper-eutectic alloys, their position off the cloud of points shows that the correlation applies better to near-eutectic alloys. Such a correlation, if confirmed by further data, should be of significant help for melt preparation before casting.

Formation of chunky graphite is known to be strongly affected by low level additions, such as Sb that is used to get rid of it and Ce which has the opposite effect. Accordingly, the V_V values were reported as function of the ratio Sb/Ce in a previous work [5] showing that a ratio higher than 0.8 could ensure castings free of CHG. This result agrees with previous conclusion by Tsumura et al. [10]. Going further in this line, Fig. 6 shows that the ratio (Sb+La)/(Mg+Ce) may be more relevant, it defines an envelop that shows a clear decrease of V_V when the value of the ratio increases. This feature is similar to what was obtained with the ratio Sb/Ce, but the number of points defining the envelop was observed to be higher with this new ratio than with the previous one. It is seen however that there are still quite a number of points showing a large range of V_V results at the minimum value (Sb+La)/(Mg+Ce)≈0.05. This is seen as the indication that better control of melt chemistry should be performed for a full mastering of chunky graphite formation.

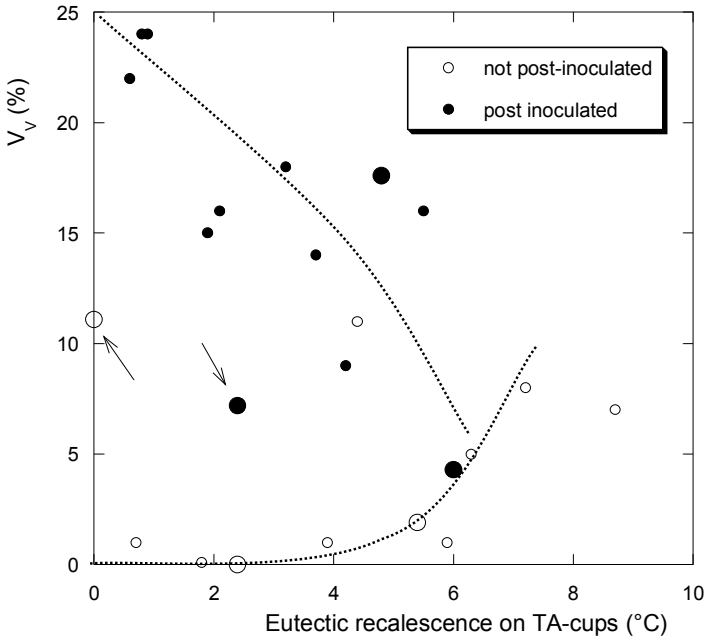

Fig. 5. Plot of V_V versus ΔT from TA cups. The arrows show points related to hypo- and hyper-eutectic alloys.

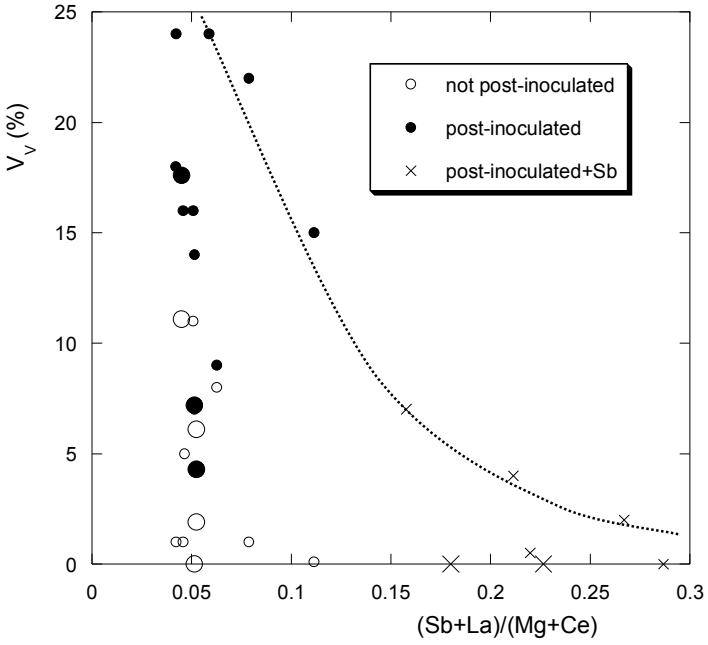

Fig. 6. Correlation between V_V fraction and several minor elements existing in the melt.

Conclusions

This work has demonstrated the detrimental effect of increasing the carbon equivalent of nodular cast irons on chunky graphite formation. Such an effect may be essentially "mechanistic", in that hypoeutectic alloys do contain less eutectic, while hypereutectic alloys present less austenite dendrites and show higher nodule counts. This latter feature agrees with previous reports that have shown that increase of nodule count through post-inoculation does lead to higher tendency for chunky graphite formation. Some correlations between eutectic recalescence in cast blocks and in TA cups that have been described previously for near-eutectic alloys appear to be less appropriate for hypo- or hyper-eutectic alloys. The sensitivity of the alloys to the presence of low level elements

and impurities has been stressed again, and this is in this line, i.e. a better control of "active" elements, that further studies should be performed for an improved understanding of the conditions leading to chunky graphite formation.

Acknowledgements

This paper is based on work supported by the Industry Department of the Spanish Government (PROFIT FIT-030000-2007-94).

References

[1] H.W. Hoover Jr., AFS Trans. Vol. 102 (1986), p. 601

[2] A. Javaid and C.R. Loper Jr.: AFS Trans. Vol. 103 (1995), p. 135

[3] P.C. Liu, C.L. Li, D.H. Wu and C.R. Loper: AFS Trans. Vol. 111 (1983), p. 119

[4] I. Asenjo, P. Larrañaga, J. Sertucha, R. Suárez, J.-M. Gomez, I. Ferrer and J. Lacaze: Int. J. Cast Met. Res. Vol. 20 (2007), p. 319

[5] P. Larrañaga, I. Asenjo, J. Sertucha, R. Suárez and J. Lacaze: Metall. Mater. Trans. A, Vol. 40A (2009), p. 654

[6] J. Sertucha, R. Suárez, I. Asenjo, P. Larrañaga, J. Lacaze, I. Ferrer and S. Armendariz: ISIJ Int. Vol. 49 (2009), p. 220-228

[7] P. Larrañaga, I. Asenjo, J. Sertucha, R. Suarez, I. Ferrer and J. Lacaze: Int. J. Cast Met. Res., Vol. 22 (2009), p. 192

[8] M. Castro, M. Herrera, M. M. Cisneros, G. Lesoult and J. Lacaze: Int. J. Cast Met. Res. Vol. 11 (1999), p. 369

[9] R. Källborn, K. Hamberg, M. Wessén and L. E. Björkegren: Mat. Sci. Eng. A, Vol. 413-414 (2005), p. 346

[10] O. Tsumura, Y. Ichinomiya, H. Narita, T. Miyamoto, T. Takenouchi: IMONO, Vol. 67 (1995), p. 540